Fixing Two-Nucleon Weak-Axial Coupling $L_{1,A}$ From $\mu^- d$ Capture

Jiunn-Wei Chen,[1] Takashi Inoue,[1,2] Xiangdong Ji,[3] and Yingchuan Li[3]

[1]*Department of Physics, National Taiwan University, Taipei, Taiwan 10617*
[2]*Department of Physics, Shophia University, Chiyoda-ku, Tokyo 102-8554, Japan*
[3]*Department of Physics, University of Maryland, College Park, Maryland 20742*

(Dated: June 1, 2005)

We calculate the muon capture rate on the deuteron to next-to-next-to-leading order in the pionless effective field theory. The result can be used to constrain the two-nucleon isovector axial coupling $L_{1,A}$ to ± 2 fm^3 if the muon capture rate is measured to 2% level. From this, one can determine the neutrino-deuteron break up reactions and the pp-fusion cross section in the sun to a same level of accuracy.

The strong evidence of neutrino oscillations observed at the Sudbury Neutrino Observatory (SNO) [1] is based on detecting the ^{8}B solar neutrino flux through the following three reactions:

$$
\begin{aligned}
&\nu_e + d \to p + p + e^- \quad &(\text{CC}),\\
&\nu_x + d \to p + n + \nu_x \quad &(\text{NC}),\\
&\nu_x + e^- \to \nu_x + e^- \quad &(\text{ES}).
\end{aligned}
\tag{1}
$$

The charged current (CC) reaction involves only the electron neutrinos, while the neutral current (NC) reaction and elastic scattering (ES) involve all the active neutrinos ($x = e, \mu, \tau$). The ν_e and ν_x fluxes are found to be significantly different[1]. Further detailed measurements of the fluxes could sharpen the constraints to neutrino oscillation parameters and provide precision tests to the standard solar model [2]. However, while the ES cross section is known to high accuracy, the CC and NC cross sections have hadronic uncertainties. As shown by Butler, Chen and Kong [3], the dominant uncertainties in low energy CC and NC cross sections comes from the coupling of a two-body isovector axial current, $L_{1,A}$, in pionless effective field theory (EFT($\not\pi$)). The potential model results of Refs. [4] and [5] can be reproduced by different choices of $L_{1,A}$, indicating that the $\sim 5\%$ difference between the models comes from the different assumptions about the short-distance nuclear physics. There are other interesting weak reactions involving the same two-body current, for example, the pp and pep fusion processes ($pp \to de^+\nu_e$, $ppe^- \to d\nu_e$) which power the sun [6, 7]. It is one of the great current interests to measure these neutrino fluxes to further test the standard solar model.

Recently much effort has been going into determining the effective two-body axial current interaction[8]. Butler, Chen, and Vogel attempted to fix $L_{1,A}$ from reactor antineutrino-deuteron breakup reactions, and they found $L_{1,A} = 3.6 \pm 5.5$ fm^3 [8]. Chen, Heeger, and Robertson obtained $L_{1,A} = 4.0 \pm 6.3$ fm^3 by using the ES data of SNO and Super-Kamiokande(SK) to calibrate SNO's CC and NC rates [9]. In Ref. [10], Park et al. used a hybrid approach to fix a two-body coupling $\hat{d}_R$ from the tritium β decay and predicted the pp fusion rate with a small error. When compared with the EFT($\not\pi$) calculation [7], their result yields $L_{1,A} = 3.7 \pm 3.5$ fm^3. A similar tritium β decay constraint using potential model yields $L_{1,A} = 4.2 \pm 2.5$ fm^3[11].

In this paper we aim to make a high-precision determination of $L_{1,A}$ from the $\mu^- d$ capture process

$$
\mu^- + d \to \nu_\mu + n + n \ , \tag{2}
$$

by calculating the rate to next-to-next-to leading order (N^{2}LO) in EFT($\not\pi$). The $\mu^- d$ capture rate has been measured previously by different groups with rather different results $\Gamma^{\exp} = 470 \pm 29\ s^{-1}$ [12] and $\Gamma^{\exp} = 409 \pm 40\ s^{-1}$ [13]. A measurement of this rate with 1% precision is under investigation at PSI [14]. An earlier potential model calculation [15] gave $\Gamma = 397 \sim 400\ s^{-1}$. More recently, the hybrid approach mentioned above gave $\Gamma = 386 \pm 5\ s^{-1}$ [16].

A concern in applying EFT($\not\pi$) to the $\mu^- d$ capture is that the energy transfer into the hadronic system might be too large to apply EFT($\not\pi$). However, as shown in Ref.[16] and also in this calculation, the contribution to the total rate from high-energy neutrons is small, and it is possible to impose a neutron energy cut to isolate the low-energy ($\lesssim 10 - 20$ MeV) neutron events without significantly increasing the statistical errors [8, 14].

Effective field theory is useful when low and high energy scales in the problem are widely separated. For low-energy processes, short-distance physics can be taken into account by local operators in an effective lagrangian involving only low-energy degrees of freedom. For $\nu(\bar{\nu}) - d$ scattering with neutrino energy below 20 MeV and $\mu^- d$ capture with small final-state neutron energy, the pion and other meson exchanges are not dynamical degrees of freedom, and their physics can be captured by contact interactions involving nucleons and the external currents. To make predictions with controlled precision, calculations are done with the perturbative expansion parameter

$$
Q \equiv \frac{(1/a_{nn}^{(^1S_0)}, \gamma, p)}{\Lambda} \ , \tag{3}
$$

which is the ratio of light to heavy scales. The light scales include the inverse S-wave neutron-neutron scattering length $1/a_{nn}^{(^1S_0)} = -10.6$ MeV in the $^1S_0$ channel, the deuteron binding momentum $\gamma = 45.7$ MeV in the $^3S_1$ channel, and typical nucleon momentum p in the system. The heavy scale Λ is set by the pion mass m_π. This EFT($\not\pi$) (see e.g. [17]) and its dibaryon version [18, 19] have been applied successfully to many processes involving the deuteron, including electro-magnetic processes such as Compton scattering $\gamma d \to \gamma d$ [20, 21], $np \to d\gamma$ relevant to the big-bang nucleonsynthesis [22, 23], weak processes such as νd reactions for SNO physics[3], the solar pp fusion process [6, 7], and parity violating observables [24]. For reviews on three-body systems, see [25].

The effective Lagrangian for the CC weak interaction is given by $\mathcal{L}^{CC} = -\sqrt{\omega_i} G_F V_{ud} l_+^\mu J_\mu^- / \sqrt{2} + \text{h.c.}$, where $G_F = 1.166 \times 10^{-5}\text{GeV}^{-2}$ is the Fermi coupling constant and $\omega_i = 1.024$ is the (inner) electromagnetic radiative correction [26] arizes from the running of G_F from the weak scale to ~ 1 GeV. $l_+^\mu = \overline{\nu}_\mu \gamma^\mu (1-\gamma_5)\mu$ is the leptonic current. The quark current $J_\mu^- = V_\mu^- - A_\mu^- = (V_\mu^1 - A_\mu^1) - i(V_\mu^2 - A_\mu^2)$ contains both vector and axial-vector interactions, where the superscripts 1 and 2 are the isospin indices. At the scale relevant to nuclear physics, the quark current need be matched to a hadronic current which in general contains one-nucleon, two-nucleon, etc., operators.

Up to the order of our interest, the one-body isovector vector and axial vector currents are

$$
\begin{aligned}
V_{(1)}^{0,a} &= N^\dagger \frac{\tau^a}{2}\left(1 + \frac{1}{6}\langle r^2\rangle_c^{I=1} \overline{\nabla}^2\right) N \\
V_{(1)}^{k,a} &= \frac{i}{2M_N} N^\dagger \overleftrightarrow{\nabla}_k \frac{\tau^a}{2} N - \frac{\mu^{(1)}}{M_N}\epsilon_{kij} N^\dagger \sigma_i \overline{\nabla}_j \frac{\tau^a}{2} N\ , \\
A_{(1)}^{0,a} &= \frac{i g_A}{2M_N} N^\dagger \vec{\sigma}\cdot \overleftrightarrow{\nabla} \frac{\tau^a}{2} N \\
&\quad - \frac{1}{4M_N^2} N^\dagger G_p\left(\overline{\nabla}^2\right) \overline{\partial_0}\vec{\sigma}\cdot\overline{\nabla}\frac{\tau^a}{2} N\ , \\
A_{(1)}^{k,a} &= g_A N^\dagger \sigma_k \frac{\tau^a}{2}\left(1 + \frac{1}{6}\langle r^2\rangle_A^{I=1}\overline{\nabla}^2\right) N \\
&\quad + \frac{1}{4M_N^2} N^\dagger G_p\left(\overline{\nabla}^2\right)\overline{\nabla}_k \vec{\sigma}\cdot\overline{\nabla}\frac{\tau^a}{2} N\ ,
\end{aligned}
\tag{4}
$$

where $\overline{\nabla} = \overleftarrow{\nabla} + \overrightarrow{\nabla}$, $\overline{\partial_0} = \overleftarrow{\partial_0} + \overrightarrow{\partial_0}$, and $\overleftrightarrow{\nabla} = \overleftarrow{\nabla} - \overrightarrow{\nabla}$. The superscript a is the isospin index, $\mu^{(1)} = (\mu_p - \mu_n)/2 = 2.353$, is the isovector nucleon magnetic moment. Isovector Dirac charge radius $\langle r^2\rangle_c^{I=1} = \langle r^2\rangle_c^p - \langle r^2\rangle_c^n = 0.873$ fm^2, and the isovector axial-charge radius $\langle r^2\rangle_A^{I=1} \simeq 0.45$ fm^2. We have neglected terms of order p^2/M_N^2 or even $\mu^{(1)}p^2/M_N^2$. The pseudoscalar form factor is, to a good approximation, dominated by the pion-pole $G_p(q^2) = \frac{4M_N^2 g_A}{M_\pi^2 - q^2}$ whose q^2 dependence will not be expanded because the momentum transfer $|\mathbf{q}|$ is of order muon mass M_μ with low energy final state neutrons. The G_p contribution to the axial current is counted of order Q.

The lowest dimensional two-body isovector currents, in the dibaryon version of EFT($\not\pi$), relevant to the $\mu^- d$ capture process are

$$
\begin{aligned}
V_{(2)}^{k,a} &= \frac{L_1^{db}}{M_N\sqrt{r^{(^3S_1)} r_{nn}^{(^1S_0)}}}\epsilon_{kij} t_i^\dagger \overline{\nabla}_j s_a + \text{h.c.}\ , \\
A_{(2)}^{k,a} &= \frac{L_{1,A}^{db}}{M_N\sqrt{r^{(^3S_1)} r_{nn}^{(^1S_0)}}}\Big(t_k^\dagger s_a \\
&\quad + \frac{G_p}{4M_N^2 g_A} t_j^\dagger \overline{\nabla}_j \overline{\nabla}_k s_a\Big) + \text{h.c.},
\end{aligned}
\tag{5}
$$

where t_i and s_a are interpolating dibaryon fields for the two-nucleon $^3S_1$ and $^1S_0$ states, respectively. The second term in $A_{(2)}^{k,a}$ is induced by the G_p term in the one-body current. $r^{(^3S_1)} = 1.764$ fm and $r_{nn}^{(^1S_0)} = 2.8$ fm are the effective ranges in triplet and two-neutron singlet channels, respectively. L_1^{db} and $L_{1,A}^{db}$ are coupling constants in dibaryon formalism. The vector current is N^{2}LO and its coupling $L_1^{db} = -4.08$ fm has been determined by the rate of $n + p \to d + \gamma$ near threshold. The axial current is NLO, and its coupling $L_{1,A}^{db}$ is proportional to the renormalization-scale-μ-independent $\tilde{L}_{1,A}$ in Ref. [3] as $L_{1,A}^{db} = \frac{M_N}{2\pi}\tilde{L}_{1,A}$, through which $L_{1,A}^{db}$ is related to the μ-dependent $L_{1,A}(\mu)$ in Ref. [3]. The numerical relation between $L_{1,A}^{db}$ and $L_{1,A}(\mu)$ is $L_{1,A}^{db} = -13.8 + 0.28 L_{1,A}(M_\pi)$, where $L_{1,A}(M_\pi)$ is in units of fm^3 and has a natural size ~ 6 fm^3.

The $\mu^- d$ atom has a ground state with a hyperfine structure, corresponding to the total angular momentum $F = 3/2$ and $F = 1/2$. The $\mu^- d$ capture process is known to take place almost uniquely from the doublet $F = 1/2$ state, because the electromagnetic decay from $F = 3/2$ to $F = 1/2$ is much faster than the capture process. The differential capture rate for muon and deuteron in their specific polarization states can be written in terms of leptonic tensor $l^{\mu\nu}$ and hadronic tensor $W_{\mu\nu}$ as

$$
\frac{d\Gamma(S,\hat{\xi})}{dE d\Omega} = \frac{\omega_i G_F^2 |V_{ud}|^2 E |\psi(0)|^2}{32\pi^2 M_\mu (1 + \frac{M_\mu}{M_d})} l^{\mu\nu}(S) W_{\mu\nu}(\hat{\xi}), \tag{6}
$$

where the $|\psi(0)|^2 = \frac{1}{\pi}\left(\alpha_{\text{em}}\frac{M_\mu M_d}{M_\mu + M_d}\right)^3$ is the $1S$-state wave-function-at-origin-squared, E is the outgoing neutrino energy, and M_d is the mass of the deuteron.

The capture rate depends on the polarization vector of the muon S_μ and the deuteron polarization vector $\hat{\xi}$. The doublet capture rate can be obtained from the subtraction of the quadruplet capture rate from the unpolarized capture rate $d\Gamma \equiv d\Gamma_{1/2} = 3\ d\Gamma_{\text{unpol.}} - 2\ d\Gamma_{3/2}$. The leptonic tensor is given by $l^{\mu\nu}(S) = 4(k^\mu k'^\nu + k'^\mu k^\nu - k\cdot k' g^{\mu\nu} + i\epsilon^{\mu\nu\rho\sigma}k_\rho k'_\sigma) - 4M_\mu(S^\mu k'^\nu + k'^\mu S^\nu - k'\cdot S g^{\mu\nu} + i\epsilon^{\mu\nu\rho\sigma}S_\rho k'_\sigma)$, where $k = (M_\mu, \vec{0})$ and $k' = (E, \vec{k'})$, with $E = |\vec{k'}|$, are the four-momenta of initial muon and final ν_μ, respectively. The hadronic tensor can be obtained from the imaginary part of the forward matrix element of the time-ordering product of two weak charged currents,

$$W_{\mu\nu}(\hat{\xi}) = \frac{1}{\pi}\mathrm{Im}\left[\int d^4x e^{iqx} T\langle d|J^{+}_{\mu}(x)J^{-}_{\nu}(0)|d\rangle\right], \quad (7)$$

where $q_\mu = k_\mu - k'_\mu$, and $|d\rangle \equiv |d(P,\hat{\xi})\rangle$ is momentum P and polarization $\hat{\xi}$ dependent deuteron state, with $P = (M_d, \vec{0})$.

The diagrams contributing to $W_{\mu\nu}(\hat{\xi})$ up to N^{2}LO are shown in Fig. 1. A straightforward calculation finds for the $F = 1/2$ state capture

$$\begin{aligned}\frac{d\Gamma}{dE} &= \frac{\omega_i G_F^2|V_{ud}|^2E^2|\psi(0)|^2}{2\pi(1+\frac{M_\mu}{M_d})}\frac{1}{1-\varepsilon\gamma r^{(^3S_1)}}\left[\left(F_{1a}-\frac{F_2}{2}\right)\right.\\ &\times\left(3G_V^2 - 2(G_V-G_A)^2 - \varepsilon\frac{4g_A(1-g_A)M_\mu E}{3(M_\pi^2-q^2)}\right.\\ &\left.+\varepsilon\mu^{(1)}\frac{8(1-g_A)E}{3M_N}\right) + \left(F_{1a}-\frac{F_2}{6}+\frac{2}{3}F_{3a}\right)\\ &\times\left(9G_A^2 - \varepsilon\frac{6g_A^2M_\mu E}{M_\pi^2-q^2}+\varepsilon^2\frac{g_A^2E^4}{(M_\pi^2-q^2)^2}\right)\\ &+(10F_{1a}-F_2+8F_{3b})\frac{\varepsilon^2{\mu^{(1)}}^2E^2}{3M_N^2}\\ &+\left(F_{1a}-\frac{F_2}{6}+\frac{2}{3}F_{3c}\right)12\varepsilon g_A\mu^{(1)}\frac{E}{M_N}\\ &-(F_{1a}+F_{3c})\frac{8\varepsilon^2g_A\mu^{(1)}E^3}{3M_N(M_\pi^2-q^2)}\\ &\left.+F_{1b}\varepsilon^2E\left(\frac{14}{3}g_A^2+\frac{16}{3}g_A+2\right)\right] \quad (8)\end{aligned}$$

where $G_V = 1+\varepsilon^2\frac{1}{6}\langle r^2\rangle_c^{I=1}q^2$ is the Dirac form factor, and $G_A = g_A(1+\varepsilon^2\frac{1}{6}\langle r^2\rangle_c^{I=1}q^2)$ is the axial form factor. The ε is formally introduced to keep track of the Q expansion. After expanded in ε and truncated at ε^2, the N^{2}LO result is obtained by setting $\varepsilon = 1$. The functions $F_{1a,1b}$, F_2, and $F_{3a,3b,3c}$ are from diagrams (a), (b), and (c), respectively, in Fig. 1

$$\begin{aligned}F_{1a} &= \frac{2M_Np\gamma}{\pi(M_N^2\Delta_E^2-p^2E^2)}\\ F_{1b} &= \frac{\gamma}{\pi E^3}\left[\frac{2M_NEp\Delta_E}{M_N^2\Delta_E^2-p^2E^2}+\ln\left(\frac{M\Delta_E-pE}{M\Delta_E+pE}\right)\right]\\ F_2 &= \frac{4\gamma}{\pi\Delta_EE}\tanh^{-1}\left(\frac{Ep}{M_N\Delta_E}\right)\\ F_{3a} &= \frac{2\gamma M_N^2}{\pi^2E^2}\mathrm{Im}\left\{G_1^2A^{(^1S_0)}(p)\right\}\\ F_{3b} &= \frac{2\gamma M_N^2}{\pi^2E^2}\mathrm{Im}\left\{G_2^2A^{(^1S_0)}(p)\right\}\\ F_{3c} &= \frac{2\gamma M_N^2}{\pi^2E^2}\mathrm{Im}\left\{G_1G_2A^{(^1S_0)}(p)\right\}, \quad (9)\end{aligned}$$

with the re-scattering amplitude in the singlet channel as $A^{(^1S_0)}(p) = -\frac{4\pi}{M_N}(\frac{1}{a_{nn}^{(^1S_0)}} - \varepsilon\frac{1}{2}r_{nn}^{(^1S_0)}p^2+ip)^{-1}$, and

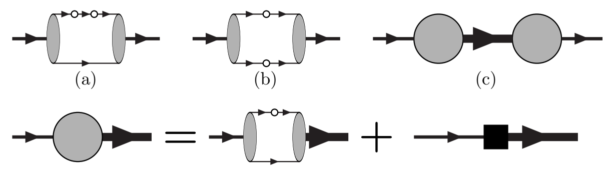

FIG. 1: Diagrams contributing to $W_{\mu\nu}(\hat{\xi})$ up to N^{2}LO. The lines inside the loop are the nucleon propagators, and the thin and thick lines outside represent the triplet and singlet dibaryon fields, respectively. The small open circle represents the insertion of hadronic one-body current. In diagram (c), the large gray circle indicates the two possible hadronic current insertions shown in the second row where the dark square denotes the two-body current associated with $L_{1,A}$ and L_1.

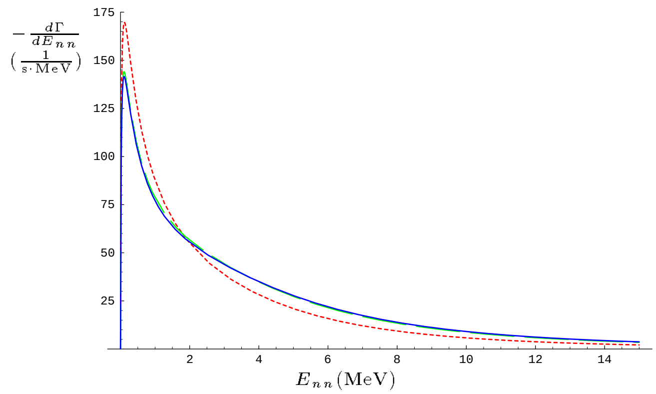

FIG. 2: The differential capture rate $d\Gamma/dE_{nn}$ calculated using $L_{1,A} = 6$ fm^3. The doted line is the LO result, the dashed line is the NLO result, while the solid line is the N^{2}LO result.

functions $G_{1,2}$ are defined as $G_1 = \tan^{-1}(\frac{E}{2(\gamma-ip)}) + \varepsilon\frac{E}{4M_Ng_A}L_{1,A}^{db}$ and $G_2 = \tan^{-1}(\frac{E}{2(\gamma-ip)})+\varepsilon\frac{E}{4\mu^{(1)}}L_1^{db}$. The energy injection into the two-neutron system is $\Delta_E \equiv M_\mu - E - (M_n - M_p)$ with $M_n - M_p = 1.293$ MeV the mass split between neutron and proton. The relative momentum between the two final-state neutrons is $2p$, with $p = \sqrt{M_N\Delta_E - \gamma^2 - E^2/4}$.

In Fig. 2 we show the differential rate $d\Gamma/dE_{nn}$ in terms of the relative motion energy $E_{nn} = 2(\sqrt{M_N^2+p^2} - M_N)$ of two final-state neutrons in the region where the EFT($\not\pi$) calculation is most reliable. It is clear from the figure that the differential rate in the energy region $E_{nn} \geq 10$ MeV is very small, and is negligible for $E_{nn} \geq 15$ MeV. By comparing the results of LO, NLO, and N^{2}LO, we find good convergence of the expansion.

In the case that a neutron energy cut can be imposed on experimental data [14], it is possible to define and measure the integrated capture rate up to a threshold energy $E_{nn}^{\rm th}$

$$\Gamma(E_{nn}^{\rm th}) \equiv -\int_0^{E_{nn}^{\rm th}}\frac{d\Gamma}{dE_{nn}}dE_{nn}. \quad (10)$$

The result up to 30 MeV is shown in Fig. 3. In the whole energy region, the NLO contribution is less than 10% of

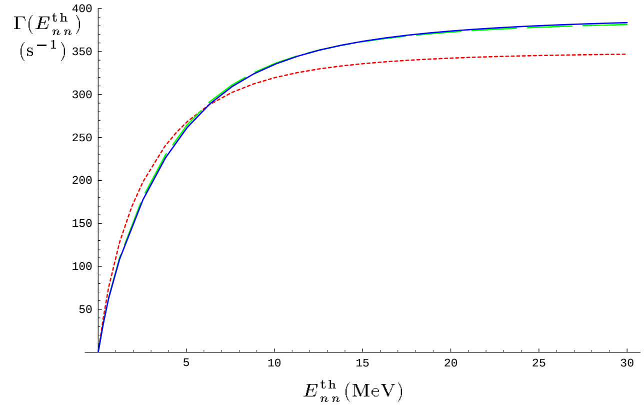

FIG. 3: The integrated capture rate $\Gamma(E_{nn}^{\text{th}})$ calculated using $L_{1,A} = 6$ fm^3 for the relative energy E_{nn}^{th} of the two neutrons up to 30 MeV. The doted, dashed, and solid lines correspond to LO, NLO, and N^{2}LO results, respectively.

the LO contribution, while the N^{2}LO contribution is less than 1%. This small size of N^{2}LO contribution is due to the cancellation between unpolarized and $F = 3/2$ contributions at N^{2}LO. This cancellation do not exist at LO, because the LO $F = 3/2$ contribution is suppressed by the $(G_V - G_A)^2$ factor. The theoretical error of our calculation is therefore at $2 \sim 3\%$ level, which translates into an error in fitted $L_{1,A}$ of the size 2 fm^3. Direct computation shows the N^{3}LO final state P-wave re-scattering only contributes $\sim 1\%$. Furthermore, the result is insensitive to the few percent uncertainty in $a_{nn}^{(^1S_0)}$. Choosing $L_{1,A} = 5.6$ fm^3, the energy dependence of our result matches the previous hybrid calculation very well [16].

To extract $L_{1,A}$ from experimental data, it is useful to provide the dependence of the rate on $L_{1,A}$

$$\Gamma(E_{nn}^{\text{th}}) = a(E_{nn}^{\text{th}}) + b(E_{nn}^{\text{th}}) L_{1,A}, \tag{11}$$

where $L_{1,A}$ is in unit of fm^3. The energy-cut dependent functions $a(E_{nn}^{\text{th}})$ and $b(E_{nn}^{\text{th}})$ for a set of E_{nn}^{th}s are listed in the Table 1, from which we observe that, for the whole range of E_{nn}^{th}, the size of $b(E_{nn}^{\text{th}})$ is about $1.3 \sim 1.5\%$ of the size of $a(E_{nn}^{\text{th}})$. This shows how an error in capture rate is translated into an uncertainty of $L_{1,A}$.

Table 1:
Coefficients functions $a(E_{nn}^{\text{th}})$ and $b(E_{nn}^{\text{th}})$ for specific values of two-neutron relative energy E_{nn}^{th} from the EFT($\not\pi$) calculation.

E_{nn}^{th}(MeV)	5.0	10.0	15.0	20.0
$a(E_{nn}^{\text{th}})(\text{s}^{-1})$	239.2	308.0	332.0	342.3
$b(E_{nn}^{\text{th}})(\text{s}^{-1}\text{fm}^{-3})$	3.3	4.2	4.7	4.9

In summary, we calculated the $\mu^- d$ capture rate using EFT($\not\pi$) to N^{2}LO. The major goal is to fix the two-nucleon isovector axial coupling constant $L_{1,A}$ from future precision experimental data. An experimental result on the integrated rate up to some neutron energy E_{nn}^{th} with a 2% error should be able to, though comparison with our calculation with theoretical error 2-3%, fix the $L_{1,A}$ with error ± 2.0 fm^3. This in turn allows us to determine the neutrino deuteron breakup cross section and the pp fusion rate in the sun to 2-3%.

This work was supported by the U. S. Department of Energy via grant DE-FG02-93ER-40762 and the NSC of Taiwan. We thank S. Ando, D.W. Hertzog, P. Kammel, K. Kubodera, and T.-S. Park for helpful discussions.

[1] Q.R. Ahmad *et al.*, Phys. Rev. Lett. **87**, 071301 (2001); **89**, 011301 (2002); **89**, 011302 (2002).
[2] J.N. Bahcall, A.M. Serenelli, and S. Basu, Astrophys. J. 621, L85 (2005).
[3] M.N. Butler and J.W. Chen, Nucl. Phys. **A675**, 575 (2000); M.N. Butler, J.W. Chen, and X. Kong, Phys. Rev. **C63**, 035501 (2001).
[4] S. Ying, W.C. Haxton and E.M. Henley, Phys. Rev. **C45**, 1982 (1992); Phys. Rev. **D40**, 3211 (1989)
[5] S. Nakamura, T. Sato, V. Gudkov and K. Kubodera, Phys. Rev. **C63**, 034617 (2001)
[6] X. Kong and F. Ravndal, Nucl. Phys. **A656**, 421 (1999); **A665**, 137 (2000); Phys. Lett. **B470**, 1 (1999); Phys. Rev. **C64**, 044002 (2001).
[7] M. Butler and J.W. Chen, Phys. Lett. **B520**, 87 (2001).
[8] M. Butler, J.W. Chen, and P. Vogel, Phys. Lett. **B549** 26 (2002).
[9] J.W. Chen, K.M. Heeger, and R.G.H. Robertson, Phys. Rev. **C67**, 025801 (2003).
[10] T.-S. Park et al., nucl-th/0106025; nucl-th/0107012.
[11] R. Schiavilla et al. Phys. Rev. **C58**, 1263 (1998).
[12] G. Bardin et al., Nucl. Phys. **A453** 591 (1986).
[13] M. Cargelli et al., in: M. Morita, H. Ejiri, H. Ohtsubo, T. Sato (Eds.), Proceedings of the XXIII Yamada Conference on Nuclear Weak Processes and Nuclear Structure, Osaka, 1989, World Scientific, Singapore, P. 115 (1989).
[14] P. Kammel *et al.*, nucl-ex/0202011; nucl-ex/0304019.
[15] N. Tatara, Y. Kohyama, K. Kubodera, Phys. Rev. **C42**, 1694 (1990)
[16] S. Ando, T.S. Park, K.Kubodera and F. Myhrer, Phys. Lett. **B533**, 25 (2002).
[17] J.W. Chen, G. Rupak, and M.J. Savage, Nucl. Phys. **A653** 386 (1999)
[18] D. B. Kaplan, Nucl. Phys. **B494**, 471 (1997).
[19] S. R. Beane and M. J. Savage, Nucl. Phys. **A694**, 511, (2001).
[20] H.W.Griesshammer and G. Rupak, Phys. Lett. **B529**, 57 (2002).
[21] J.W. Chen, X. Ji, and Y. Li, nucl-th/0408003, to appear in Phys. Lett. **B**; Phys. Rev. **C71**, 044321 (2005).
[22] J.W. Chen and M.J. Savage, Phys. Rev. **C60**, 065205 (1999).
[23] G. Rupak, Nucl. Phys. **A678**, 405 (2000).
[24] M.J. Savage, Nucl. Phys. **A695**, 365 (2001).
[25] P. F. Bedaque and U. van Kolck, Ann. Rev. Nucl. Part. Sci. **52**, 339 (2002); E. Braaten and H.-W. Hammer, cond-mat/0410417.
[26] A. Sirlin, Rev. Mod. Phys. **50**, 573 (1978).